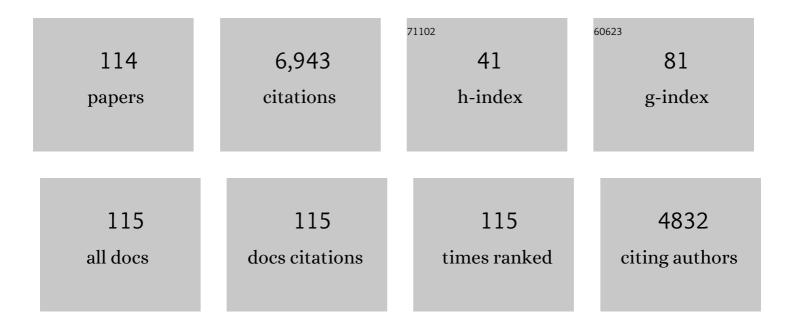
Christiaan van der Tol

List of Publications by Year in descending order

Source: https://exaly.com/author-pdf/3585367/publications.pdf Version: 2024-02-01



| # | Article | IF | CITATIONS |
|----|--|------|-----------|
| 1 | Linking chlorophyll a fluorescence to photosynthesis for remote sensing applications: mechanisms and challenges. Journal of Experimental Botany, 2014, 65, 4065-4095. | 4.8 | 770 |
| 2 | An integrated model of soil-canopy spectral radiances, photosynthesis, fluorescence, temperature and energy balance. Biogeosciences, 2009, 6, 3109-3129. | 3.3 | 440 |
| 3 | Remote sensing of solar-induced chlorophyll fluorescence (SIF) in vegetation: 50†years of progress. Remote Sensing of Environment, 2019, 231, 111177. | 11.0 | 372 |
| 4 | Models of fluorescence and photosynthesis for interpreting measurements of solarâ€induced chlorophyll fluorescence. Journal of Geophysical Research G: Biogeosciences, 2014, 119, 2312-2327. | 3.0 | 281 |
| 5 | Quantifying Vegetation Biophysical Variables from Imaging Spectroscopy Data: A Review on Retrieval Methods. Surveys in Geophysics, 2019, 40, 589-629. | 4.6 | 265 |
| 6 | Far-red sun-induced chlorophyll fluorescence shows ecosystem-specific relationships to gross primary production: An assessment based on observational and modeling approaches. Remote Sensing of Environment, 2015, 166, 91-105. | 11.0 | 263 |
| 7 | Estimation of vegetation photosynthetic capacity from spaceâ€based measurements of chlorophyll fluorescence for terrestrial biosphere models. Global Change Biology, 2014, 20, 3727-3742. | 9.5 | 260 |
| 8 | Forest productivity and water stress in Amazonia: observations from GOSAT chlorophyll fluorescence. Proceedings of the Royal Society B: Biological Sciences, 2013, 280, 20130171. | 2.6 | 245 |
| 9 | Global sensitivity analysis of the SCOPE model: What drives simulated canopy-leaving sun-induced fluorescence?. Remote Sensing of Environment, 2015, 166, 8-21. | 11.0 | 211 |
| 10 | Model-based analysis of the relationship between sun-induced chlorophyll fluorescence and gross primary production for remote sensing applications. Remote Sensing of Environment, 2016, 187, 145-155. | 11.0 | 185 |
| 11 | Linking canopy scattering of far-red sun-induced chlorophyll fluorescence with reflectance. Remote Sensing of Environment, 2018, 209, 456-467. | 11.0 | 172 |
| 12 | Plant functional traits and canopy structure control the relationship between photosynthetic <scp>CO</scp> ₂ uptake and farâ€red sunâ€induced fluorescence in a Mediterranean grassland under different nutrient availability. New Phytologist, 2017, 214, 1078-1091. | 7.3 | 158 |
| 13 | A model for chlorophyll fluorescence and photosynthesis at leaf scale. Agricultural and Forest Meteorology, 2009, 149, 96-105. | 4.8 | 157 |
| 14 | Fluspect-B: A model for leaf fluorescence, reflectance and transmittanceÂspectra. Remote Sensing of Environment, 2016, 186, 596-615. | 11.0 | 147 |
| 15 | Integration of soil moisture in SEBS for improving evapotranspiration estimation under water stress conditions. Remote Sensing of Environment, 2012, 121, 261-274. | 11.0 | 117 |
| 16 | Estimating crop primary productivity with Sentinel-2 and Landsat 8 using machine learning methods trained with radiative transfer simulations. Remote Sensing of Environment, 2019, 225, 441-457. | 11.0 | 112 |
| 17 | Evaluating the predictive power of sun-induced chlorophyll fluorescence to estimate net photosynthesis of vegetation canopies: A SCOPE modeling study. Remote Sensing of Environment, 2016, 176, 139-151. | 11.0 | 111 |
| 18 | Simulations of chlorophyll fluorescence incorporated into the <scp>C</scp> ommunity <scp>L</scp> and <scp>M</scp> odel version 4. Global Change Biology, 2015, 21, 3469-3477. | 9.5 | 95 |

| # | Article | IF | CITATIONS |
|----|--|------|-----------|
| 19 | Extending Fluspect to simulate xanthophyll driven leaf reflectance dynamics. Remote Sensing of Environment, 2018, 211, 345-356. | 11.0 | 92 |
| 20 | On the relationship between sub-daily instantaneous and daily total gross primary production: Implications for interpreting satellite-based SIF retrievals. Remote Sensing of Environment, 2018, 205, 276-289. | 11.0 | 91 |
| 21 | A model and measurement comparison of diurnal cycles of sun-induced chlorophyll fluorescence of crops. Remote Sensing of Environment, 2016, 186, 663-677. | 11.0 | 80 |
| 22 | Hyperspectral radiative transfer modeling to explore the combined retrieval of biophysical parameters and canopy fluorescence from FLEX – Sentinel-3 tandem mission multi-sensor data. Remote Sensing of Environment, 2018, 204, 942-963. | 11.0 | 80 |
| 23 | Fluorescence Correction Vegetation Index (FCVI): A physically based reflectance index to separate physiological and non-physiological information in far-red sun-induced chlorophyll fluorescence. Remote Sensing of Environment, 2020, 240, 111676. | 11.0 | 78 |
| 24 | Remote sensing of plant-water relations: An overview and future perspectives. Journal of Plant Physiology, 2018, 227, 3-19. | 3.5 | 70 |
| 25 | Global transpiration data from sap flow measurements: the SAPFLUXNET database. Earth System Science Data, 2021, 13, 2607-2649. | 9.9 | 65 |
| 26 | Estimation of forest above-ground biomass using multi-parameter remote sensing data over a cold and arid area. International Journal of Applied Earth Observation and Geoinformation, 2012, 14, 160-168. | 2.8 | 62 |
| 27 | The mSCOPE model: A simple adaptation to the SCOPE model to describe reflectance, fluorescence and photosynthesis of vertically heterogeneousÂcanopies. Remote Sensing of Environment, 2017, 201, 1-11. | 11.0 | 62 |
| 28 | Analysis of Red and Far-Red Sun-Induced Chlorophyll Fluorescence and Their Ratio in Different Canopies Based on Observed and Modeled Data. Remote Sensing, 2016, 8, 412. | 4.0 | 59 |
| 29 | Groundwater and unsaturated zone evaporation and transpiration in a semi-arid open woodland. Journal of Hydrology, 2017, 547, 54-66. | 5.4 | 56 |
| 30 | Remote Sensing of Grass Response to Drought Stress Using Spectroscopic Techniques and Canopy Reflectance Model Inversion. Remote Sensing, 2016, 8, 557. | 4.0 | 54 |
| 31 | Using reflectance to explain vegetation biochemical and structural effects on sun-induced chlorophyll fluorescence. Remote Sensing of Environment, 2019, 231, 110996. | 11.0 | 52 |
| 32 | Heatwave breaks down the linearity between sunâ€induced fluorescence and gross primary production. New Phytologist, 2022, 233, 2415-2428. | 7.3 | 51 |
| 33 | Impact of land use and land cover transitions and climate on evapotranspiration in the Lake Naivasha Basin, Kenya. Science of the Total Environment, 2019, 682, 19-30. | 8.0 | 50 |
| 34 | The scattering and re-absorption of red and near-infrared chlorophyll fluorescence in the models Fluspect and SCOPE. Remote Sensing of Environment, 2019, 232, 111292. | 11.0 | 49 |
| 35 | EAGLE 2006 – Multi-purpose, multi-angle and multi-sensor in-situ and airborne campaigns over grassland and forest. Hydrology and Earth System Sciences, 2009, 13, 833-845. | 4.9 | 48 |
| 36 | Spatioâ€Temporal Convergence of Maximum Daily Lightâ€Use Efficiency Based on Radiation Absorption by Canopy Chlorophyll. Geophysical Research Letters, 2018, 45, 3508-3519. | 4.0 | 48 |

| # | Article | IF | CITATIONS |
|----|--|------|-----------|
| 37 | Integrating satellite optical and thermal infrared observations for improving daily ecosystem functioning estimations during a drought episode. Remote Sensing of Environment, 2018, 209, 375-394. | 11.0 | 45 |
| 38 | Reference crop evapotranspiration derived from geo-stationary satellite imagery: a case study for the Fogera flood plain, NW-Ethiopia and the Jordan Valley, Jordan. Hydrology and Earth System Sciences, 2010, 14, 2219-2228. | 4.9 | 44 |
| 39 | FluorWPS: A Monte Carlo ray-tracing model to compute sun-induced chlorophyll fluorescence of three-dimensional canopy. Remote Sensing of Environment, 2016, 187, 385-399. | 11.0 | 43 |
| 40 | Quantifying the uncertainty in estimates of surface–atmosphere fluxes through joint evaluation of the SEBS and SCOPE models. Hydrology and Earth System Sciences, 2013, 17, 1561-1573. | 4.9 | 42 |
| 41 | An evaluation of SCOPE: A tool to simulate the directional anisotropy of satellite-measured surface temperatures. Remote Sensing of Environment, 2015, 158, 362-375. | 11.0 | 42 |
| 42 | Exploring the physiological information of Sun-induced chlorophyll fluorescence through radiative transfer model inversion. Remote Sensing of Environment, 2018, 215, 97-108. | 11.0 | 41 |
| 43 | Impact of climate change-induced alterations in peatland vegetation phenology and composition on carbon balance. Science of the Total Environment, 2022, 827, 154294. | 8.0 | 41 |
| 44 | Estimating zero-plane displacement height and aerodynamic roughness length using synthesis of LiDAR and SPOT-5 data. Remote Sensing of Environment, 2011, 115, 2330-2341. | 11.0 | 40 |
| 45 | Estimating montane forest above-ground biomass in the upper reaches of the Heihe River Basin using Landsat-TM data. International Journal of Remote Sensing, 2014, 35, 7339-7362. | 2.9 | 40 |
| 46 | Modelling sun-induced fluorescence and photosynthesis with a land surface model at local and regional scales in northern Europe. Biogeosciences, 2017, 14, 1969-1987. | 3.3 | 40 |
| 47 | SCOPE 2.0: a model to simulate vegetated land surface fluxes and satellite signals. Geoscientific Model Development, 2021, 14, 4697-4712. | 3.6 | 39 |
| 48 | Average wet canopy evaporation for a Sitka spruce forest derived using the eddy correlation-energy balance technique. Journal of Hydrology, 2003, 276, 12-19. | 5.4 | 38 |
| 49 | Quantitative Estimation of Fluorescence Parameters for Crop Leaves with Bayesian Inversion. Remote Sensing, 2015, 7, 14179-14199. | 4.0 | 35 |
| 50 | Multiple-constraint inversion of SCOPE. Evaluating the potential of GPP and SIF for the retrieval of plant functional traits. Remote Sensing of Environment, 2019, 234, 111362. | 11.0 | 35 |
| 51 | Coupling socio-economic factors and eco-hydrological processes using a cascade-modeling approach. Journal of Hydrology, 2014, 518, 49-59. | 5.4 | 33 |
| 52 | Modeling forest above-ground biomass dynamics using multi-source data and incorporated models: A case study over the qilian mountains. Agricultural and Forest Meteorology, 2017, 246, 1-14. | 4.8 | 32 |
| 53 | Unraveling the physical and physiological basis for the solar- induced chlorophyll fluorescence and photosynthesis relationship using continuous leaf and canopy measurements of a corn crop. Biogeosciences, 2021, 18, 441-465. | 3.3 | 32 |
| 54 | Retrieval of canopy component temperatures through Bayesian inversion of directional thermal measurements. Hydrology and Earth System Sciences, 2009, 13, 1249-1260. | 4.9 | 31 |

| # | Article | IF | CITATIONS |
|----|--|------|-----------|
| 55 | Variance-based sensitivity analysis of BIOME-BGC for gross and net primary production. Ecological Modelling, 2014, 292, 26-36. | 2.5 | 28 |
| 56 | The SPART model: A soil-plant-atmosphere radiative transfer model for satellite measurements in the solar spectrum. Remote Sensing of Environment, 2020, 247, 111870. | 11.0 | 28 |
| 57 | Validation of remote sensing of bare soil ground heat flux. Remote Sensing of Environment, 2012, 121, 275-286. | 11.0 | 26 |
| 58 | Representing the root water uptake process in the Common Land Model for better simulating the energy and water vapour fluxes in a Central Asian desert ecosystem. Journal of Hydrology, 2013, 502, 145-155. | 5.4 | 26 |
| 59 | Estimating photosynthetic capacity from leaf reflectance and Chl fluorescence by coupling radiative transfer to a model for photosynthesis. New Phytologist, 2019, 223, 487-500. | 7.3 | 26 |
| 60 | Systematic Orbital Geometry-Dependent Variations in Satellite Solar-Induced Fluorescence (SIF) Retrievals. Remote Sensing, 2020, 12, 2346. | 4.0 | 25 |
| 61 | Characterisation of hydroclimatological trends and variability in the Lake Naivasha basin, Kenya. Hydrological Processes, 2015, 29, 3276-3293. | 2.6 | 24 |
| 62 | Downscaling of far-red solar-induced chlorophyll fluorescence of different crops from canopy to leaf level using a diurnal data set acquired by the airborne imaging spectrometer HyPlant. Remote Sensing of Environment, 2021, 264, 112609. | 11.0 | 24 |
| 63 | Testing three approaches to estimate soil evaporation through a dry soil layer in a semi-arid area. Journal of Hydrology, 2018, 567, 405-419. | 5.4 | 23 |
| 64 | Optimal inverse estimation of ecosystem parameters from observations of carbon and energy fluxes. Biogeosciences, 2019, 16, 77-103. | 3.3 | 23 |
| 65 | Extending the SCOPE model to combine optical reflectance and soil moisture observations for remote sensing of ecosystem functioning under water stress conditions. Remote Sensing of Environment, 2019, 221, 286-301. | 11.0 | 23 |
| 66 | Discrete anisotropic radiative transfer modelling of solar-induced chlorophyll fluorescence: Structural impacts in geometrically explicit vegetation canopies. Remote Sensing of Environment, 2021, 263, 112564. | 11.0 | 22 |
| 67 | Growing season net ecosystem <scp>CO</scp> ₂ exchange of two desert ecosystems with alkaline soils in Kazakhstan. Ecology and Evolution, 2014, 4, 14-26. | 1.9 | 21 |
| 68 | Global Sensitivity Analysis of the SCOPE Model in Sentinel-3 Bands: Thermal Domain Focus. Remote Sensing, 2019, 11, 2424. | 4.0 | 21 |
| 69 | Effect of sub-layer corrections on the roughness parameterization of a Douglas fir forest. Agricultural and Forest Meteorology, 2012, 162-163, 115-126. | 4.8 | 19 |
| 70 | The Complicate Observations and Multi-Parameter Land Information Constructions on Allied Telemetry Experiment (COMPLICATE). PLoS ONE, 2015, 10, e0137545. | 2.5 | 19 |
| 71 | Nitrogen and Phosphorus effect on Sun-Induced Fluorescence and Gross Primary Productivity in Mediterranean Grassland. Remote Sensing, 2019, 11, 2562. | 4.0 | 19 |
| 72 | Energy partitioning and its controls over a heterogeneous semiâ€arid shrubland ecosystem in the Lake Naivasha Basin, Kenya. Ecohydrology, 2016, 9, 1358-1375. | 2.4 | 18 |

| # | Article | IF | CITATIONS |
|----|---|------|-----------|
| 73 | The influence of long-term changes in canopy structure on rainfall interception loss: a case study in Speulderbos, the Netherlands. Hydrology and Earth System Sciences, 2018, 22, 3701-3719. | 4.9 | 18 |
| 74 | Hyplant-Derived Sun-Induced Fluorescence—A New Opportunity to Disentangle Complex Vegetation Signals from Diverse Vegetation Types. Remote Sensing, 2019, 11, 1691. | 4.0 | 18 |
| 75 | Uncertainty analysis of gross primary production partitioned from net ecosystem exchange measurements. Biogeosciences, 2016, 13, 1409-1422. | 3.3 | 16 |
| 76 | A Bayesian approach to estimate sensible and latent heat over vegetated land surface. Hydrology and Earth System Sciences, 2009, 13, 749-758. | 4.9 | 15 |
| 77 | senSCOPE: Modeling mixed canopies combining green and brown senesced leaves. Evaluation in a Mediterranean Grassland. Remote Sensing of Environment, 2021, 257, 112352. | 11.0 | 15 |
| 78 | Topography induced spatial variations in diurnal cycles of assimilation and latent heat of Mediterranean forest. Biogeosciences, 2007, 4, 137-154. | 3.3 | 14 |
| 79 | Optimum vegetation characteristics, assimilation, and transpiration during a dry season: 1. Model description. Water Resources Research, 2008, 44, . | 4.2 | 14 |
| 80 | Reprint of: Estimation of forest above-ground biomass using multi-parameter remote sensing data over a cold and arid area. International Journal of Applied Earth Observation and Geoinformation, 2012, 17, 102-110. | 2.8 | 14 |
| 81 | Retrieval of land surface properties from an annual time series of Landsat TOA radiances during a drought episode using coupled radiative transfer models. Remote Sensing of Environment, 2020, 238, 110917. | 11.0 | 14 |
| 82 | Integrated modeling of canopy photosynthesis, fluorescence, and the transfer of energy, mass, and momentum in the soil–plant–atmosphere continuum (STEMMUS–SCOPE v1.0.0). Geoscientific Model Development, 2021, 14, 1379-1407. | 3.6 | 14 |
| 83 | Contact and directional radiative temperature measurements of sunlit and shaded land surface components during the SEN2FLEX 2005 campaign. International Journal of Remote Sensing, 2008, 29, 5183-5192. | 2.9 | 13 |
| 84 | Decoupling of a Douglas fir canopy: a look into the subcanopy with continuous vertical temperature profiles. Biogeosciences, 2020, 17, 6423-6439. | 3.3 | 13 |
| 85 | Simulation of Forest Evapotranspiration Using Time-Series Parameterization of the Surface Energy Balance System (SEBS) over the Qilian Mountains. Remote Sensing, 2015, 7, 15822-15843. | 4.0 | 12 |
| 86 | Meteorological controls on evapotranspiration over a coastal salt marsh ecosystem under tidal influence. Agricultural and Forest Meteorology, 2019, 279, 107755. | 4.8 | 12 |
| 87 | Improved retrieval of land surface biophysical variables from time series of Sentinel-3 OLCI TOA spectral observations by considering the temporal autocorrelation of surface and atmospheric properties. Remote Sensing of Environment, 2021, 256, 112328. | 11.0 | 12 |
| 88 | Bayesian integration of flux tower data into a process-based simulator for quantifying uncertainty in simulated output. Geoscientific Model Development, 2018, 11, 83-101. | 3.6 | 11 |
| 89 | Characterization of a Highly Biodiverse Floodplain Meadow Using Hyperspectral Remote Sensing within a Plant Functional Trait Framework. Remote Sensing, 2016, 8, 112. | 4.0 | 10 |
| 90 | Unified Four-Stream Radiative Transfer Theory in the Optical-Thermal Domain with Consideration of Fluorescence for Multi-Layer Vegetation Canopies. Remote Sensing, 2020, 12, 3914. | 4.0 | 10 |

| # | Article | IF | CITATIONS |
|-----|--|-------------------|---------------|
| 91 | On the seasonal relation of sun-induced chlorophyll fluorescence and transpiration in a temperate mixed forest. Agricultural and Forest Meteorology, 2021, 304-305, 108386. | 4.8 | 10 |
| 92 | An Overview of the Regional Experiments for Land-atmosphere Exchanges 2012 (REFLEX 2012) Campaign. Acta Geophysica, 2015, 63, 1465-1484. | 2.0 | 9 |
| 93 | Spatial Patterns and Temporal Stability of Throughfall in a Mature Douglas-fir Forest. Water (Switzerland), 2018, 10, 317. | 2.7 | 9 |
| 94 | Modelling hourly evapotranspiration in urban environments with SCOPE using open remote sensing and meteorological data. Hydrology and Earth System Sciences, 2022, 26, 1111-1129. | 4.9 | 8 |
| 95 | Automated Directional Measurement System for the Acquisition of Thermal Radiative Measurements of Vegetative Canopies. Sensors, 2009, 9, 1409-1422. | 3.8 | 7 |
| 96 | A simple method using climatic variables to estimate canopy temperature, sensible and latent heat fluxes in a winter wheat field on the North China Plain. Hydrological Processes, 2009, 23, 665-674. | 2.6 | 7 |
| 97 | An Analysis of Turbulent Heat Fluxes and the Energy Balance During the REFLEX Campaign. Acta Geophysica, 2015, 63, 1516-1539. | 2.0 | 5 |
| 98 | Google Earth Engine Sentinel-3 OLCI Level-1 Dataset Deviates from the Original Data: Causes and Consequences. Remote Sensing, 2021, 13, 1098. | 4.0 | 5 |
| 99 | Year-long, broad-band, microwave backscatter observations of an alpine meadow over the Tibetan Plateau with a ground-based scatterometer. Earth System Science Data, 2021, 13, 2819-2856. | 9.9 | 5 |
| 100 | Can we retrieve vegetation photosynthetic capacity paramter from solar-induced fluorescence?. , 2016, , . | | 3 |
| 101 | Dynamic analysis and modeling of Forest above-ground biomass. , 2014, , . | | 2 |
| 102 | Modeling Reflectance, Fluorescence and Photosynthesis: Development of the Scope Model. , 2018, , . | | 2 |
| 103 | Modeling hydrological response to land use/cover change: case study of Chirah Watershed (Soan) Tj ETQq1 1 C | .784314 rg 1.3 | gBT_/Overloci |
| 104 | Quantitative global mapping of terrestrial vegetation photosynthesis: The Fluorescence Explorer (FLEX) mission. , 2017, , . | | 1 |
| 105 | Broadband Full Polarimetric Scatterometry for Monitoring Soil Moisture and Vegetation Properties Over a Tibetan Meadow. , 2018, , . | | 1 |
| 106 | Mapping of biophysical and biochemical properties of coastal tidal wetland habitats with Landsat 8. Journal of Applied Remote Sensing, 2021, 15, . | 1.3 | 1 |
| 107 | Scaling photosynthetic function and CO2 dynamics from leaf to canopy level for maize – dataset combining diurnal and seasonal measurements of vegetation fluorescence, reflectance and vegetation indices with canopy gross ecosystem productivity. Data in Brief, 2021, 39, 107600. | 1.0 | 1 |
| 108 | Regional forest above-ground biomass retrieval by optimized k-NN algorithm in Northeast China. , 2013, | | 0 |

7

,.

| # | ARTICLE | IF | CITATIONS |
|-----|--|----|-----------|
| 109 | Global sensitivity analysis of the A-SCOPE model in support of future FLEX fluorescence retrievals. , 2014, , . | | 0 |
| 110 | Sensitivity of scope modelled GPP and fluorescence for different plant functional types. , 2014, , . | | 0 |
| 111 | Photosynthesis-Sun Induced Fluorescence Relationship in a Mediterranean Grassland. , 2018, , . | | 0 |
| 112 | A Spectral Invariant Approach to Modelling Radiative Transfer Of Sun-Induced Chlorophyll Fluorescence. , 2018, , . | | 0 |
| 113 | Estimation of Vegetation Functioning in a Drought Episode from Optical and Thermal Remote Sensing. , 2018, , . | | 0 |
| 114 | Multi-model Approach for Spatial Evapotranspiration Mapping: Comparison of Models Performance for Different Ecosystems. , 2014, , 285-305. | | 0 |